Optimizing the photon flux of double optical gated high-order harmonic spectra

Hiroki Mashiko, Steve Gilbertson, Chengquan Li, Eric Moon, and Zenghu Chang*
J. R. Macdonald Laboratory, Department of Physics, Kansas State University, Manhattan, Kansas 66506, USA
(Received 3 April 2008; published 30 June 2008)

The combination of polarization gating and two-color gating is a promising approach to generate single isolated attosecond pulses with multicycle pump lasers. We searched the phase-matching conditions for high-order harmonic generation with such a double optical gating using 0.85 mJ, 8 fs laser pulses centered at 790 nm. At the optimized gas target location and pressure, the single extreme ultraviolet pulse energy is 6.5 nJ for argon and 170 pJ for neon, which are much higher then those generated with conventional polarization gating. In addition, the carrier-envelope phase effects with a 2π periodicity were attained when the highest extreme ultraviolet photon flux was produced, indicating the robustness of the double optical gating.

DOI: 10.1103/PhysRevA.77.063423 PACS number(s): 32.80.Qk, 42.65.Re, 42.65.Ky

I. INTRODUCTION

Single isolated attosecond pulses are powerful tools for studying electron dynamics in atoms, molecules, and solids [1]. In recent years, such pulses have been produced by high-order harmonic generation with few-cycle laser pulses [2–4]. However, the low photon flux of such extreme ultraviolet (xuv) pulses limited their applications, especially for studying nonlinear physics. The photon flux of attosecond pulses is determined by the pump laser energy and the conversion efficiency of the generation scheme. The pulse energy of the ~5 fs, carrier-envelope (CE) phase controlled lasers used in Refs. [3,4] was <0.4 mJ. When the pump laser is linearly polarized, only the cutoff region of the high-order harmonic spectrum is filtered out [3], while all the photons in the broad plateau are damped. In this case, the energy of the 170 as pulses at center wavelength of 13 nm was 16 pj from a neon gas target. Even shorter pulses (130 as) were generated by the polarization gating (PG) technique [5]. Experimentally, conventional PG pulses have been generated by combining two counter-rotating circularly polarized laser pulses with a proper delay [6–10]. Only the laser energy inside the polarization gate contributes to the xuv generation while other portions of the pump laser energy are wasted. The attosecond pulse energy with such a scheme was ~70 pJ at center wavelength of 45 nm using argon and ~3 pJ at center wavelength of 25 nm using neon target gas [11].

Recently, a double optical gating (DOG) technique that combines the PG and two-color gating was demonstrated to generate xuv supercontinua that can support single isolated pulses [12–14]. The main advantage of this scheme is that multi cycle pump lasers can be used. It is much easier to develop high-energy long pulse pump lasers which are important for achieving high power attosecond pulses. Furthermore, the daily operation of such lasers is much simpler than running the two-cycle lasers used previously for attosecond pulse generation. For the same pump laser pulse duration, the DOG is more efficient than conventional PG. This is due to reduced depletion of the ground state population by the pulse outside the gate [15]. Previously, 140 pJ per xuv pulse were generated by DOG after an aluminum filter (900 pJ before)[14]. For given pump laser parameters and target gas pressure, the highest achievable photon flux of the high-order harmonic pulses is determined by the balance between the coherence length, absorption length, and the media length. This has been studied extensively for long pulse driving lasers [16–18].

So far, the most energetic xuv pulses were generated using 30 fs lasers. By loosely focusing the pump laser beam to a long gas cell, 25 nJ per harmonic order at 13 nm from neon gas were produced using 30 fs, 50 mJ lasers centered at 800 nm [19]. High-order harmonic generation with two-color field has been extensive studied since the first demonstration [20–23]. The xuv pulses with 600 pJ energy centered at 21.6 nm wavelength were obtained by a 30 fs two-color pump laser from helium gas [24]. Recently, the two-color gating has been used in the study of both attosecond pulse train [25,26] and single attosecond pulses [27]. The added second harmonic field in the DOG helps the phase-matching process by suppressing the ionization caused by the leading edge of the PG field.

For conventional harmonic generation, it is well known that phase matching is affected by the location of the gas target in the laser focus region and by the gas pressure. Although the general phase-matching principle for high-order harmonic generation is also valid for generating single isolated attosecond pulses, special attention must be paid for the latter. When the photon flux of attosecond pulses is optimized, the experimental conditions should keep the correct dependence of the harmonic spectra on the CE phase of the excitation lasers. A small gas pressure-length product (1 mbar × 1 mm) was used in previous PG experiments to preserve the CE phase dependence [5,11], which is one of the reasons for the low photon flux. In this work, we searched the best target location and pressure to optimize the photon flux of the xuv supercontinua generated by the DOG scheme. At the same time, we wanted to find out whether the unique dependence of the gated xuv spectrum on the CE phase is kept at the best phase-matching conditions.

II. EXPERIMENT

Previous studies show that argon gas is the best target for efficiently generating high-order harmonics in the 25–40 nm range, while neon gas is better for generating harmonics up

*chang@phys.ksu.edu

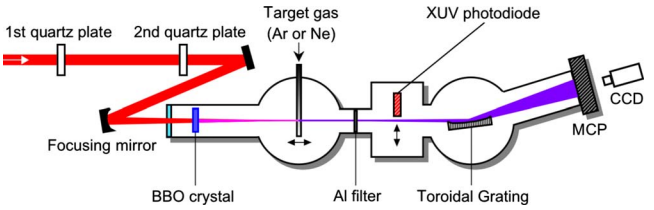

FIG. 1. (Color online) Schematic of the double optical gating setup.

to ~13 nm. These two gases are also used in our studies. The electric fields for DOG can be resolved into a driving component and an orthogonally polarized gating field. The harmonic pulse can only be generated in the one optical cycle region where the gating field is much lower than the driving field. Although DOG can be implemented with laser pulses as long as 12 fs, we chose 8 fs to increase the field strength ratio between the driving field inside the polarization gate to that of the outside, in order to suppress the unwanted ionization of the atom by the leading edge of the DOG fields. As compared to conventional PG, the DOG works for a much broader range of pump laser pulse durations. However, there is a tradeoff between pulse duration and laser-to-xuv conversion efficiency. The shorter the pulse duration is, the higher the conversion efficiency due to the reduction of the depletion of the ground state population. We chose 8 fs in this work as a compromise between the xuv photon flux and the pump laser difficulties.

The pump pulses originate in a grating-based chirped pulse amplifier [28]. The laser produces 25 fs, 2.5 mJ pulses centered at 800 nm at 1 kHz with a power stabilization feedback loop [29]. The CE phase stabilization of the oscillator was accomplished by the self-referencing technique [30,31]. The slow phase drift in the amplifier was compensated by feedback control of the grating separation [32–34]. The output beam was sent to a hollow-core fiber and chirped mirror compressor. The gas pressure inside the fiber was adjusted to obtain 8 fs pulse duration with energy of 0.85 mJ, full width at half maximum centered at 790 nm [35]. For a given pump pulse duration, the highest possible pump energy should be used to produce more attosecond photon flux. Figure 1 shows a schematic of the experimental setup. The DOG of collinear type was constructed by two birefringent quartz plates and a barium borate (BBO) crystal similar to the setup described in Ref. [14]. The first and second quartz plates have thicknesses of 270 μm and 440 μm, respectively. The first plate thickness sets the polarization gate width to 2.5 fs, i.e., one optical cycle. The optical axis of the second quartz plate and the BBO are aligned in the same direction as the polarization of the beam from the fiber. They work together to serve as a quarter wave plate and convert the two pulses from the first quartz plate into a PG pulse. The BBO crystal with thickness of 150 μm was placed inside a vacuum chamber to generate the second harmonic (SH) field that is superimposed on the PG field for DOG. The estimated pulse duration of the SH pulse is 20 fs with energy of 80 μJ [36]. A spherical mirror with focal length of 400 mm was used to focus the laser beam on the gas cell filled with argon or neon gases. The gas cell is a needle type with inner diameter of 1.4 mm and a laser drilled hole of ~200 μm diameter. The

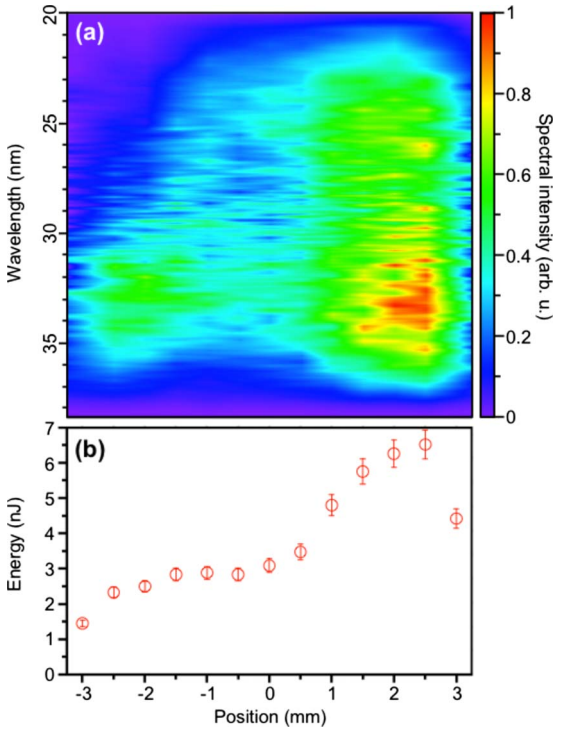

FIG. 2. (Color online) Comparison of double optical gated harmonic spectra at several locations within laser focus with argon target gas. (a) The harmonic spectrum images. (b) The open circles are pulse energy before aluminum filter.

spot sizes of the IR and SH beams were 40 μm and 30 μm at the focus position, yielding Rayleigh lengths corresponding to 6.3 mm and 7.2 mm, respectively. The peak intensities of the linear polarized portion of the IR and SH pulses at the focus were 1.9×10^{15} W/cm^2 and 1.7×10^{14} W/cm^2, respectively. The generated harmonics were sent to a transmittance calibrated aluminum filter with thickness of 200 nm. The photon flux was measured by an xuv photodiode (IRD Inc., AXUV-100). The generated harmonics were measured by a spectrometer with a toroidal grating [37].

III. RESULT AND DISCUSSION

A. Dependence of interaction gas location

In order to properly phase match the harmonic spectra, we first needed to find the best location of the gas cell within the confocal range of the fundamental laser. It is well known that the focusing geometry has a large influence on the phase matching of harmonic generation through the Gouy phase and atomic dipole phase shifts [38]. Figure 2(a) shows the harmonic spectra while scanning argon gas (backing pressure is ~90 mbar) filled interaction cell through the laser focus. The location of the cell in front of the beam focus corresponds to the negative sign, and the positive sign is opposite that. Clearly the harmonic signal shows a peak yield at a certain location of 2.5 mm after the laser focus while maintaining a continuous spectrum. Figure 2(b) shows the photon flux of harmonics measured by the xuv photodiode located after an aluminum filter. The filter was found to have a transmittance of the harmonic orders of ~10–25 % due to thin

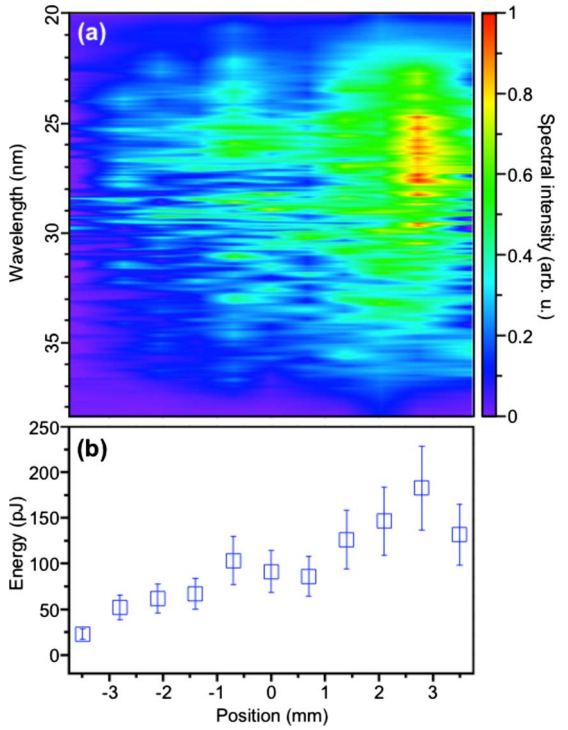

FIG. 3. (Color online) Comparison of double optical gated harmonic spectra at several locations within laser focus with neon target gas. (a) The harmonic spectrum images. (b) The open squares are pulse energy before aluminum filter.

layers of aluminum oxide on both sides such as Ref. [39]. This was used to obtain the photon flux before the aluminum filter as shown in the figure. This best location was found at 2.5 mm after the laser focus, in agreement with the location for the continuous spectrum in Fig. 2(a).

Figure 3(a) shows the harmonic spectra when scanning the location of the gas cell using neon gas (backing pressure is ~40 mbar). The best phase matching condition for a supercontinuum spectrum is 3 mm after the focus. Due to the increase in the ionization potential for neon, the plasma effects are much less as compared with that of argon gas. Figure 3(b) is the photon flux as a function of the location. The photon flux also indicates the best location is 3 mm after the focus. These results show that the optimum supercontinuum spectrum is matched to the location of the maximum photon flux.

B. Dependence of interaction gas pressure

Figure 4(a) shows the spectra for several values of the argon target gas pressure. The gas cell was kept at a constant location of 2.5 mm. As was expected, the pressure played a large role in the harmonic yield as it contributes to both the plasma density and the neutral atom response contributions of the phase matching. Through increasing pressure, we found optimal signal strength near 90 mbar in backing pressure. Figure 4(b) shows the results of the estimated harmonics photon flux as a function of the gas pressure. Again we see the peak value occurs at ~90 mbar. Under these optimal phase matching conditions, the pulse energy (open circles) was estimated at ~6.5 nJ before the aluminum filter as measured with the xuv photodiode. The solid line shows the absorption curve of residual gas between the cell and aluminum filter (length is 241 mm) inside the chamber calculated by Ref. [40], while the dashed line shows a curve corresponding to absorption inside the cell. We calculated the co-

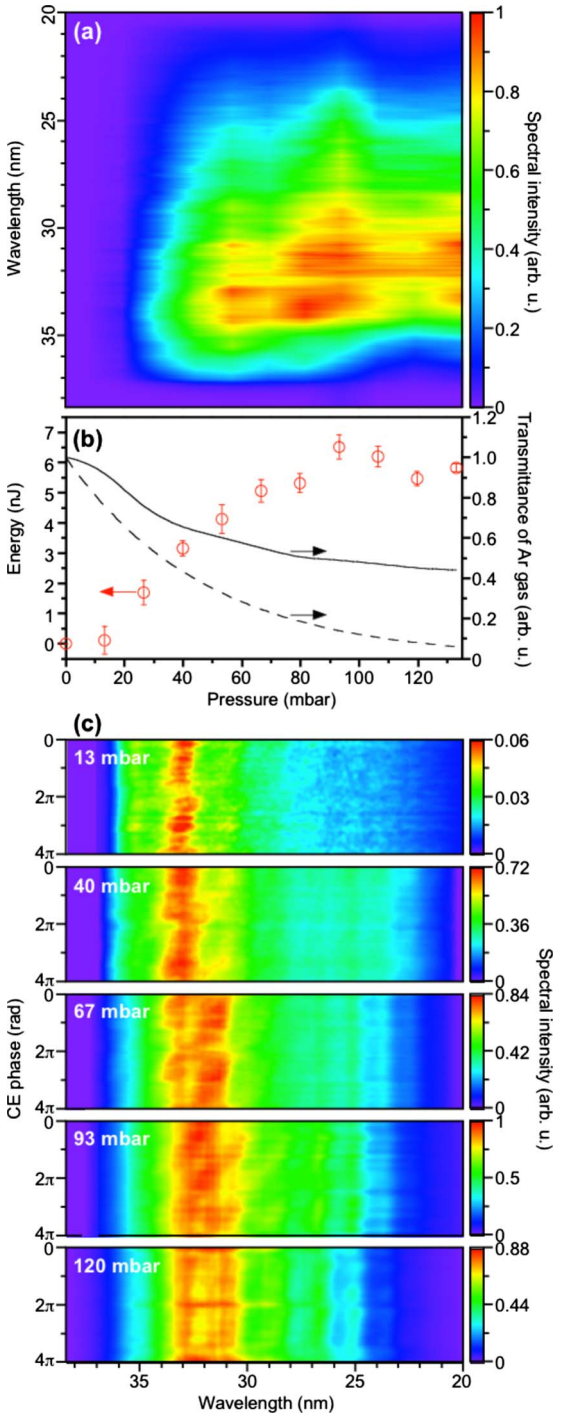

FIG. 4. (Color online) Comparison of double optical gated harmonic spectra at several pressures of argon target gas. (a) The harmonic spectrum images. (b) The open circles are pulse energy before aluminum filter. The solid and dashed lines correspond to the absorption by residual gas and plasma in the chamber and the target cell, respectively. (c) The dependence of harmonic spectra with CE phase in pressure range of 13 to 120 mbar of our backing pressure.

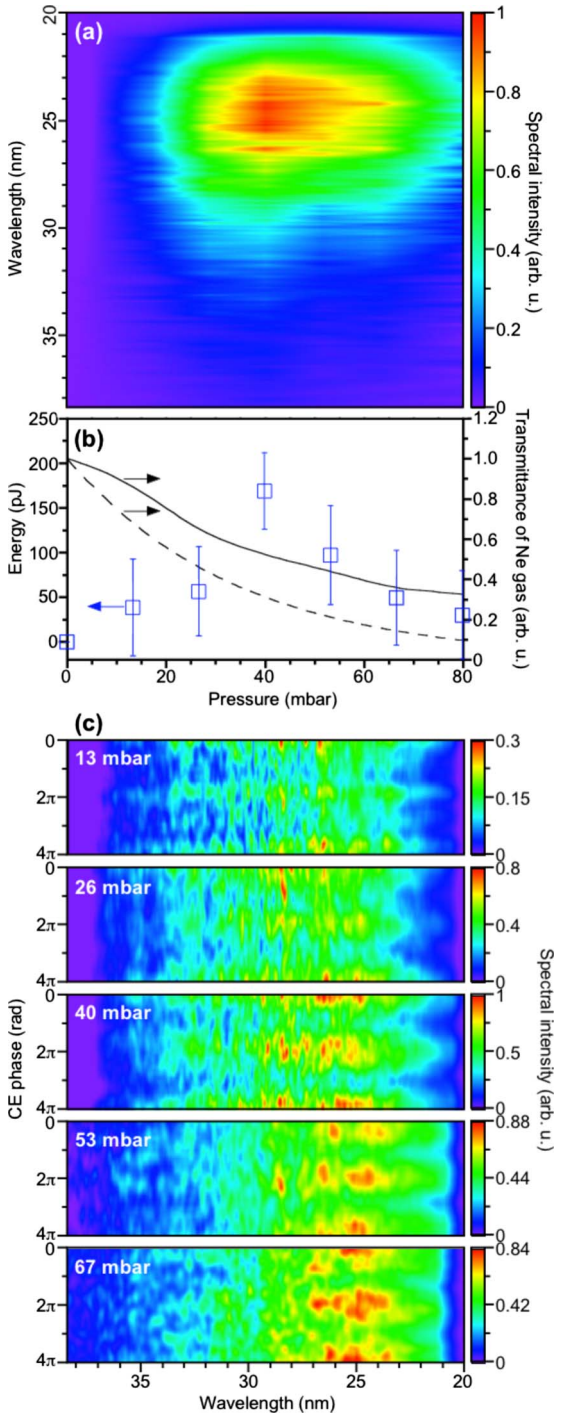

FIG. 5. (Color online) Comparison of double optical gated harmonic spectra with several pressures of neon gas. (a) The harmonic spectrum images. (b) The open squares are pulse energy before aluminum filter. The solid and dashed lines correspond to the absorption by residual gas and plasma in the chamber and the target cell, respectively. (c) The dependence of harmonic spectra with CE phase in pressure range of 13 to 67 mbar.

herence length based on our experimental results using the method described in Ref. [16] and also took into account the absorption in the chamber. The estimated coherence length was found to be ten times longer than the absorption length, indicating the phase matching is nearly optimized. The effective gas pressure within the interaction region for this calculation was estimated from our backing pressure and vacuum pump rate. This maximum energy corresponds to an estimated photon number of 9×10^{8} per pulse and a conversion efficiency of 6×10^{-6}. An interesting point can be noted here however. If we consider only the linear portion within the gate width as actually contributing to the harmonic generation (which is indeed the case), the effective conversion efficiency can be as high as 4×10^{-5}. The enhanced signal strength of the DOG pulses is explained by the reduced depletion of the target gas from the leading edge of the pulse. We observed the effect of the CE phase on the harmonic spectra under different target gas pressures as shown in Fig. 4(c). The 2π periodicity provides evidence that the spectra are harmonics of DOG pulses [13,14]. The increasing pressure did not eliminate the DOG effect, thereby demonstrating its robustness.

The optimal pressure of neon gas was found experimentally as shown in Fig. 5(a). The gas cell was ideally located 3 mm after the laser focus. The harmonic spectra are not changed much by the gas pressure scan similar to the results of argon. However, as shown in Fig. 5(b), the pulse energy (open squares) sharply decays at pressures higher than 40 mbar. The major contribution of this is strong absorption by the neon gas as shown with the solid and dashed lines corresponding to absorption from the chamber and the gas cell, respectively. The estimated coherence length is 1.5 times longer than the absorption length. The photon flux achieved at least 170 pJ pulse energy before the aluminum filter corresponding to 2×10^{7} photons per pulse and a conversion efficiency 2×10^{-7}. The effective efficiency considering only the polarization gate width contribution is 1×10^{-6}. Finally, we observed the spectra performing a CE phase scan. The distributions of the harmonics have 2π periodicity at each pressure value. From these results, the supercontinuum spectra are not influenced strongly by the pressure issue.

IV. CONCLUSION

We optimized the photon flux of the xuv supercontinua that can support single isolated attosecond pulses. The DOG harmonic signal was investigated by studying the location of the interaction region and the target gas pressure dependence using 0.85 mJ, 8 fs pump laser pulses. The maximum pulse energy achieved using argon and neon gas were 6.5 nJ and 170 pJ before the aluminum filter, respectively. The flux can be further improved by more than a factor of 2 by improving the vacuum of the target chamber. From the intense pump laser pulses with DOG, the isolated attosecond pulse energies are much higher than other reported values [3,11]. In addition, the CE phase effects with every 2π periodicity were observed under the best phase-matched conditions, indicating the robustness of the DOG.

ACKNOWLEDGMENTS

This material is supported by the NSF under Grant No. 0457269, by the U. S. Army Research Office under Grant No. W911NF-07-1-0475, and by the U.S. Department of Energy.

[1] A. Scrinzi, M. Yu Ivanov, R. Kienberger, and D. M. Villeneuve, J. Phys. B **39**, R1 (2006).
[2] S. Sartania, Z. Cheng, M. Lenzner, G. Tempea, Ch. Spielmann, F. Krausz, and K. Ferencz, Opt. Lett. **22**, 1562 (1997).
[3] M. Schultze, E. Goulielmakis, M. Uiberacker, M. Hofstetter, J. Kim, D. Kim, F. Krausz, and U. Kleineberg, New J. Phys. **9**, 243 (2007).
[4] R. Kienberger, E. Goulielmakis, M. Uiberacker, A. Baltuska, V. Yakovlev, F. Bammer, A. Scrinzi, Th. Westerwalbesloh, U. Kleineberg, U. Heinzmann, M. Drescher, and F. Krausz, Nature (London) **427**, 817 (2004).
[5] G. Sansone, E. Benedetti, F. Calegari, C. Vozzi, L. Avaldi, R. Flammini, L. Poletto, P. Villoresi, C. Altucci, R. Velotta, S. Stagira, S. De Silvestri, and M. Nisoli, Science **314**, 443 (2006).
[6] P. B. Corkum, N. H. Burnett, and M. Y. Ivanov, Opt. Lett. **19**, 1870 (1994).
[7] V. T. Platonenko and V. V. Strelkov, J. Opt. Soc. Am. B **16**, 435 (1999).
[8] O. Tcherbakoff, E. Mével, D. Descamps, J. Plumridge, and E. Constant, Phys. Rev. A **68**, 043804 (2003).
[9] B. Shan, S. Ghimire, and Zenghu Chang, J. Mod. Opt. **52**, 277 (2005).
[10] Zenghu Chang, Phys. Rev. A **70**, 043802 (2004).
[11] I. J. Sola, E. Mével, L. Elouga, E. Constant, V. Strelkov, L. Poletto, P. Villoresi, E. Benedetti, J.-P. Caumes, S. Stagira, C. Vozzi, G. Sansone, and M. Nisoli, Nat. Phys. **2**, 319 (2006).
[12] Zenghu Chang, Phys. Rev. A **76**, 051403(R) (2007).
[13] H. Mashiko, S. Gilbertson, C. Li, S. D. Khan, M. M. Shakya, E. Moon, and Zenghu Chang, Phys. Rev. Lett. **100**, 103906 (2008).
[14] S. Gilbertson, H. Mashiko, C. Li, S. D. Khan, M. M. Shakya, E. Moon, and Zenghu Chang, Appl. Phys. Lett. **92**, 071109 (2008).
[15] Zenghu Chang, Phys. Rev. A **71**, 023813 (2005).
[16] E. Constant, D. Garzella, P. Breger, E. Mével, Ch. Dorrer, C. Le Blanc, F. Salin, and P. Agostini, Phys. Rev. Lett. **82**, 1668 (1999).
[17] A. Rundquist, C. G. Durfee III, Zenghu Chang, C. Herne, S. Backus, M. M. Murnane, and H. C. Kapteyn, Science **280**, 1412 (1998).
[18] M. Schnürer, Z. Cheng, M. Hentschel, G. Tempea, P. Kálmán, T. Brabec, and F. Krausz, Phys. Rev. Lett. **83**, 722 (1999).
[19] E. J. Takahashi, Y. Nabekawa, and K. Midorikawa, Appl. Phys. Lett. **84**, 4 (2004).
[20] M. D. Perry and J. K. Crane, Phys. Rev. A **48**, R4051 (1993).
[21] H. Eichmann, A. Egbert, S. Nolte, C. Momma, B. Wellegehausen, W. Becker, S. Long, and J. K. McIver, Phys. Rev. A **51**, R3414 (1995).
[22] U. Andiel, G. D. Tsakiris, E. Cormier, and K. Witte, Europhys. Lett. **47**, 42 (1999).
[23] T. T. Liu, T. Kanai, T. Sekikawa, and S. Watanabe, Phys. Rev. A **73**, 063823 (2006).
[24] I. J. Kim, G. H. Lee, S. B. Park, Y. S. Lee, T. K. Kim, C. H. Nam, T. Mocek, and K. Jakubczak, Appl. Phys. Lett. **92**, 021125 (2008).
[25] N. Dudovich, O. Smirnova, J. Levesque, Y. Mairesse, M. Yu. Ivanov, D. M. Villeneuve, and P. B. Corkum, Nat. Phys. **2**, 781 (2006).
[26] J. Mauritsson, P. Johnsson, E. Gustafsson, A. L'Huillier, K. J. Schafer, and M. B. Gaarde, Phys. Rev. Lett. **97**, 013001 (2006).
[27] Y. Oishi, M. Kaku, A. Suda, F. Kannari, and K. Midorikawa, Opt. Express **14**, 7230 (2006).
[28] B. Shan, C. Wang, and Zenghu Chang, U.S. Patent No. 7,050,474 (23 May 2006).
[29] H. Wang, C. Li, J. Tackett, H. Mashiko, C. M. Nakamura, E. Moon, and Zenghu Chang, Appl. Phys. B: Lasers Opt. **89**, 275 (2007).
[30] D. J. Jones, S. A. Diddams, J. K. Ranka, A. Stentz, R. S. Windeler, J. L. Hall, and S. T. Cundiff, Science **288**, 635 (2000).
[31] E. Moon, C. Li, Z. Duan, J. Tackett, K. L. Corwin, B. R. Washburn, and Zenghu Chang, Opt. Express **14**, 9758 (2006).
[32] C. Li, E. Moon, and Zenghu Chang, Opt. Lett. **31**, 3113 (2006).
[33] Z. Chang, Appl. Opt. **45**, 8350 (2006).
[34] C. Li, E. Moon, H. Mashiko, C. M. Nakamura, P. Ranitovic, C. M. Maharjan, C. L. Cocke, Zenghu Chang, and G. G. Paulus, Opt. Express **14**, 11468 (2006).
[35] H. Mashiko, C. M. Nakamura, C. Li, E. Moon, H. Wang, J. Tackett, and Zenghu Chang, Appl. Phys. Lett. **90**, 161114 (2007).
[36] SNLO software website: http://www.sandia.gov/imrl/XWEB1128/snloftp.htm
[37] M. M. Shakya, S. Gilbertson, H. Mashiko, C. M. Nakamura, C. Li, E. Moon, Z. Duan, J. Tackett, and Zenghu Chang, Proc. SPIE **6703**, 67030 (2007).
[38] P. Salières, A. L'Huillier, and M. Lewenstein, Phys. Rev. Lett. **74**, 3776 (1995).
[39] F. R. Powell, P. W. Vedder, J. F. Lindblom, and S. F. Powell, Opt. Eng. (Bellingham) **26**, 614 (1990).
[40] B. L. Henke, E. M. Gullikson, and J. C. Davis, At. Data Nucl. Data Tables **54**, 181 (1993).